Thermodynamic analysis of a high temperature heat pump coupled with an organic Rankine cycle for energy storage

Lukas Lindeman[1], Violeta Sánchez-Canales[1], Laura O´Donoghue[1], Abdelrahman H. Hassan[1,2], José M. Corberán[1], Jorge Payá[1]

[1]Universitat Politècnica de València, Instituto Universitario de Investigación en Ingeniería Energética, Camino de Vera s/n, Valencia 46022, Spain, Phone: 34-96-3879124, Fax: 34-96 3879126
[2]Mechanical Power Engineering Department, Faculty of Engineering, Zagazig University, Zagazig 44519, Egypt, Phone: 20-55-2363635, Fax: 20-55-2304987
e-mail (of the first author): lindeman@kth.se

ABSTRACT

Energy storage is one of the bottlenecks to increase the share of renewable energy in electricity production. This paper presents an interesting solution, which is to produce heat at high temperature during times of excess electricity production (e.g. from wind turbines), store the heat and recover it at a later stage in order to produce electricity by means of an organic Rankine cycle (ORC). The heat production is ensured by a high temperature heat pump (HTHP), and the heat is stored in latent and sensible heat storage systems.

This work has been developed under the frame of the European project CHESTER (**C**ompressed **H**eat **E**nergy **ST**orage for **E**nergy from **R**enewable sources). A thermodynamic model has been developed using Engineering Equation Software (EES) to evaluate the system performance. This study analyzes the impact of three phase change material (PCM) with different melting temperatures (133, 149 and 183 °C), the selection of the refrigerant (dry, isentropic or wet fluid) and the choice of the thermodynamic cycle. The results indicate that isentropic fluids have the best overall system performance. Among the assessed refrigerants, R1233zd(E) is the best working fluid for the low and medium melting temperatures. For a melting temperature of 133 °C, a roundtrip efficiency of 1 can be reached if the source temperature is 75 °C. For the high temperature storage (183 °C), R141b is the best working fluid. A two-stage compression in the HTHP does not appear to be beneficial for the system, nor does the introduction of a recuperator or regenerator in the ORC cycle.

Keywords: *Thermal storage system; High temperature heat pump; organic Rankine cycle; Numerical modeling;*

1. Introduction

Carbon is the source of most electricity generation in the world today. CO_2 is released into the atmosphere whenever a carbon-based fuel (e.g coal, natural gas, crude oil) is combusted and this contributes to global warming. To reduce CO_2 emissions, the conventional carbon-based electricity generation needs to be phased out to make room for electricity generation from renewable energy sources (RES). The issue of intermittency with RES electricity generation can be mitigated by integrating energy storage solutions into the grid, and therefore storage technology is expected to play a key role in the increase of renewable technology use [4, 11].

Pumped Hydro Storage (PHS) is by far the most mature and widely used storage technique. The efficiency of PHS is usually within the range of 65-85 %. However, PHS is limited by geological constraints and it requires an appropriate elevation and a large supply of water [1].

Another option is Compressed Air Energy Storage (CAES). CAES uses excess electricity to compress air and, when electricity is needed, the gas is heated and expanded through a turbine to generate electricity. The efficiency of CAES systems are around 70%. The drawbacks of this technology are the lack of maturity compared to others, geographical restrictions, and environmental issues due to the underground storage and the necessity of using fossil fuels during the discharging process [1, 3, 4].

The concept of Pumped Thermal Energy Storage (PTES) is considered to be a promising alternative, in which the excess electricity is used during the charging process to drive a HTHP and increase the temperature of a heat source. This energy is stored in a high temperature thermal energy storage system (HT-TES) that can be latent, sensible or both, to be used later in a thermodynamic cycle to produce electrical power in periods of high demand (discharging process) [4].

This project proposes the development of a PTES system using a subcritical ORC during the discharge process. This concept is also known as CHEST (Compressed Heat Energy STorage). This work has been carried out under the frame of the European project CHESTER (under grant agreement No. 764042). The CHESTER project pursues the development and evaluation of an innovative, efficient and smart energy storage and management system to provide increased flexibility to the power grid. In addition, it will allow the integration of thermal RES such as solar, biomass, waste heat, geothermal, etc. This integration of low temperature waste heat will compensate for unavoidable exergy losses and the system can theoretically achieve a roundtrip efficiency (electrical) of over 100%. [4, 12, 13].

The main objective of the current work is to analyze the thermodynamic performance of the CHEST system for different PCM with distinct melting temperatures, working fluids, and cycle configurations.

2. The CHEST Concept

Figure 1 shows a basic scheme of the CHEST system. At times when there is a disposal of excess electricity, the low-grade thermal energy is pumped to a hotter reservoir, or HT-TES, hereby charging the CHEST system. Later, during periods of high demand, the thermal heat stored is used to operate an ORC to produce electricity. This is the discharging process.

To efficiently charge the HT-TES, the HTHP operates between evaporation temperatures of 30-100 °C and condensation temperatures up to 200 °C. Later, the fluid of the ORC system evaporates at a temperature below the melting temperature of the PCM.
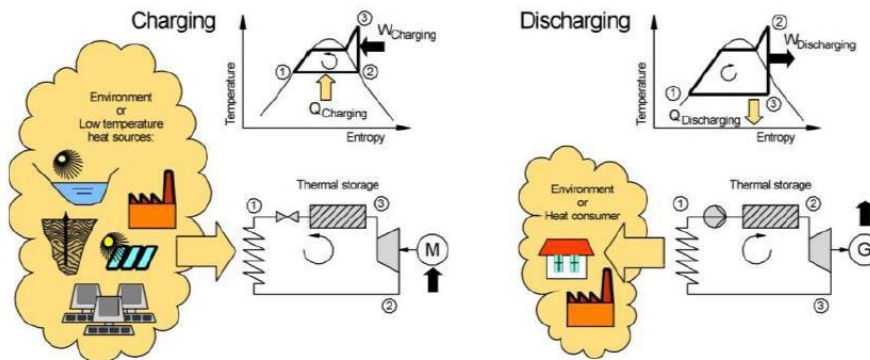
Figure 1. Basic schematic of CHEST [12]

2.1 Overall CHEST system

Figure 2 shows the detailed layout for the CHEST system. In the HTHP (left-hand-side) the compressor uses excess electricity to pump the working fluid from a low temperature heat source to the HT-TES system. After charging the HT-TES system, the working fluid is throttled down to the evaporating pressure and, when a surplus of electricity occurs again, the HTHP cycle is repeated. Figure 2 shows a single compression stage in the HTHP, however, in some cases, several compression stages have also been studied to reduce the compression ratio and the discharge temperature.
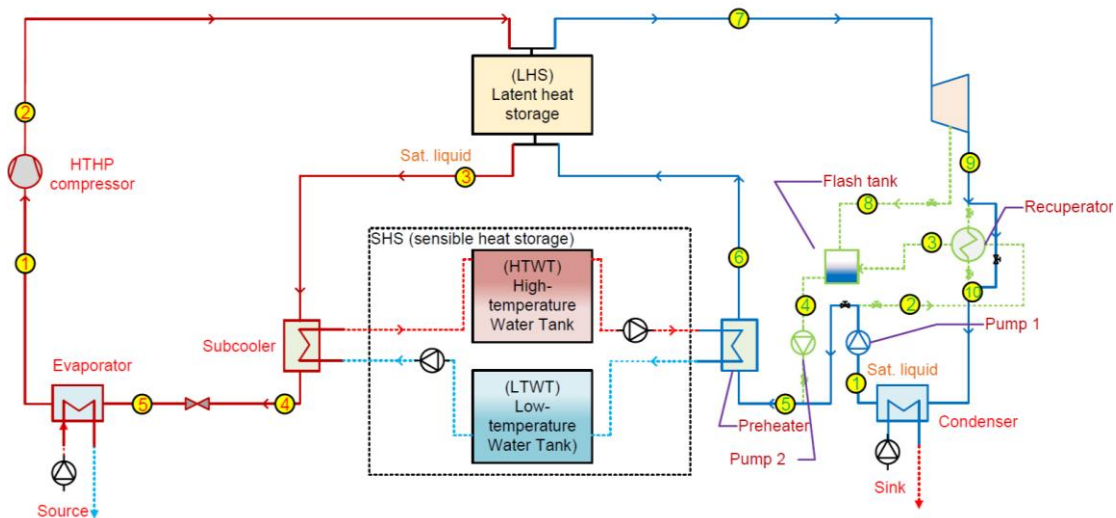

Figure 2. General layout of the CHEST system with one stage of compression in the HTHP

The HT-TES is divided into a latent heat storage (LHS) system, which consists of a tank with a PCM, and a sensible heat storage (SHS), composed of two water tanks at different temperature levels. The storage systems are explained in detail in Sections 2.2 and 2.3.

When the demand of electricity is higher than the current supply and the system has been previously charged, the heat is removed from the HT-TES and converted to electricity via the ORC cycle (right-hand-side of Figure 2). The working fluid in the ORC is firstly preheated in the SHS unit, then evaporated and superheated in the LHS unit. Secondly, it expands through the expander to generate electricity. Thirdly, it is condensed at a temperature slightly higher than the ambient sink temperature. Finally, it is pumped to the high-pressure level and the discharging cycle is repeated.

2.2 Latent heat storage (LHS) system

The LHS contains a PCM which is assumed to be constantly at the phase-change temperature. When the HTHP is functioning to charge the storage, the solid PCM melts and latent heat is stored. Later, if the ORC is working, latent heat is extracted from the LHS tank and the PCM solidifies. For an efficient storage unit, the PCM should have a high latent heat of fusion and a high thermal conductivity [2]. Considering the condensation and evaporation temperature of the HTHP and the ORC, it is necessary to find materials that have a melting temperature in an appropriate range for this application. As in Jockernhöfer et al.[4], eutectic mixtures were selected due to their high specific melting enthalpy (ΔH_{melt}) and high melting temperature (T_{melt}). In Table 1 the three PCMs, with T_{melt} in the range of 130-190 ˚C, selected for the comparison of the results of the thermodynamic analysis of the CHEST system are presented.

Table 1 Melting Temperature of selected PCMs [6]

Case	Material	T_{melt} (˚C)	Δh_{melt} (kJ/kg)
1	$LiNO_3$–KNO_3	133	150
2	KNO_2-$NaNO_3$	149	124
3	$LiOH$-$LiNO_3$	183	352

2.3 Sensible heat storage (SHS) system

The layout of the SHS can be seen in Figure 2.The SHS consists of a high temperature water tank (HTWT) and a low temperature water tank (LTWT) containing water at two different temperature levels. During the charging, the water from LTWT is pumped through the subcooler to cool down the HTHP working fluid. The outlet hot water is pumped to the HTWT where it is stored. During the discharging, the hot water is pumped to the preheater where the refrigerant used in the ORC is heated up. The cold water is then stored in the LTWT where it is kept until the next cycle.

3. Description of the Model

EES [5] has been used to develop the proposed model for the CHEST system and to run the simulations and parametric studies. This program has been chosen because it allows for simple programing, direct access to the thermal properties of a vast amount of working fluids and detailed output results and figures.

The modeling assumptions are as follows: the system works under steady state conditions; the HTHP's compressor has a constant isentropic efficiency of 0.8; the refrigerant mass flow rate, after the evaporator is 1 kg/s; there is a constant pressure drop in all heat exchangers equal to 5% of the inlet pressure; there is a fixed temperature difference at the corresponding pinch point of 5 K for all heat exchangers; a fixed value of 0.8 is used for isentropic efficiencies of ORC's expander and pump; and, finally, no heat losses in the HT-TES system, which implies that the ratio between latent and sensible heat is always the same for both HTHP and ORC.

Figure 3 shows the basic thermodynamic cycle of the charging and discharging cycles. In the charging cycle (red solid line), and more particularly in the 5-1 process, heat is transferred to the refrigerant in the HTHP from the low-temperature heat source and in 1-2 the refrigerant is compressed. Then, the processes 2-3 and 3-4 correspond, respectively, to the latent (condensation of working fluid) and sensible (subcooling of working fluid) heat transfer to the LHS and SHS systems. After this, the working fluid is expanded to the lower pressure level (4-5).

For the discharging cycle (blue dotted line), between 5-6 the working fluid in the ORC cycle is preheated using heat from the SHS. In 6-7, further heat is transferred from the LHS to the

refrigerant to evaporate and superheat it. In process 7-9, the steam is passed through an expander and electricity is generated. Finally, the steam is condensed between 9 and 1.
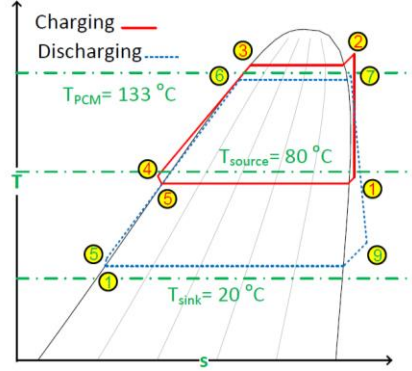

Figure 3. T-s diagram of the CHEST system

3.1 HTHP performance indicators

The coefficient of performance for HTHP (COP$_{HTHP}$) is the main indicator which is defined as:

$$COP_{HP}(-)=\frac{\dot{Q}_{HTHP,tot}}{\dot{W}_{HTHP,tot}} \tag{1}$$

, where $\dot{Q}_{HTHP,tot}$ (kW) and $\dot{W}_{HTHP,tot}$ (kW) are the total heat transferred to the HT-TES and the total electrical power consumed by the HTHP, respectively.

The volumetric heat capacity for HTHP (VHC$_{HTHP}$) is used to estimate the heat capacity per volume and is an indicator of the required compressor size. In order to have a small size of the compressor, high values of VHC$_{HTHP}$ are desirable.

$$VHC_{HTHP}(kJ/m^3)=\frac{h_2-h_4}{v_1} \tag{2}$$

v_1 (m^3/kg) is the specific volume of refrigerant at inlet of compressor and h_2 and h_4 (kJ/kg) are the enthalpies of points 2 and 4 of the diagram.

Moreover, the lubrication oils need to be stable at the maximum temperature of the compressor. Therefore, the final discharge temperature (point 2 of HTHP cycle) has also been evaluated.

3.2 ORC performance indicators

The following parameters are used to evaluate the system performance for the ORC. The thermal efficiency for ORC ($\eta_{thermal,ORC}$) is defined in Eq. (3).

$$\eta_{thermal,ORC}(-)=\frac{\dot{W}_{net,ORC}}{\dot{Q}_{in,ORC}} \tag{3}$$

$\dot{W}_{net,ORC}$ (kW) and $\dot{Q}_{in,ORC}$ (kW) are the net electrical power output and total thermal power input to the ORC, respectively

The volumetric expansion ratio for ORC (VER$_{ORC}$) is defined as follows:

$$VER_{ORC}(-)=\frac{v_9}{v_7} \tag{4}$$

, where v_7 and v_9 (m^3/kg) are the specific volumes at the inlet and outlet of the ORC's expander, respectively. In order to avoid large size expanders and a large number of stages, the VER$_{ORC}$ should be as low as possible.

5

3.3   Refrigerant selection

The refrigerants selected to carry on in the study and their properties are presented in Table 2. Three different types of fluids (wet, dry and isentropic) have been selected for analysis, depending on the slope of the saturated vapor curve on the T-s diagram which is, respectively, negative, positive or vertical. The sink temperature is expected to be similar to the ambient and, therefore, the saturation pressure has been calculated at 25 °C.

Table 2. Selected refrigerants categorized by type, normal boiling point (NBP), critical temperature (T_{crit}), pressure at 25°C ($P_{25°C}$), critical pressure (P_{crit}) and global warming potential (GWP)

Refrigerant	Type	NBP (°C)	T_{crit} (°C)	$P_{25°C}$ (kPa)	P_{crit} (kPa)	GWP
Acetone [10]	Wet	56	235	31	4700	<10
R141b [8]	Isentropic	32	204	79	4212	725
R1233zd(E) [9]	Isentropic	18	165	130	3573	<1
HFO1336mzz(Z) [14]	Dry	33	171	100	2900	2
Cyclopentane [7]	Dry	49	239	42	4571	10

Three different cases, one for each PCM proposed in Table 1, are studied, and three refrigerants (one of each type) per case are introduced, leading to a total of nine different sub-cases. The refrigerants have been selected so that their working range meets the temperature criteria of each case. The working range, in the current study, is defined as the temperature difference between the critical temperature (T_{crit}) and normal boiling point (NBP).

While T_{sink} remains the same (25 °C), the value of T_{source} has been analyzed in the range between 40 and 100 °C. Furthermore, three condensation temperatures are studied for the HTHP. Since there is a pinch point difference between the PCM and the working fluid, 5 K has been added to the melting temperature in the HTHP. The refrigerants chosen for each case are shown in Table 3.

Table 3. Refrigerant selection for Cases 1, 2, and 3

Case	T_{sink} (°C)	$T_{melt,PCM}$ (°C)	T_{cond} (°C)	Wet fluid selected	Isentropic fluid selected	Dry fluid selected
Case 1	25	133	138	Acetone	R1233zd(E)	HFO1336mzz(Z)
Case 2	25	149	154	Acetone	R1233zd(E)	HFO1336mzz(Z)
Case 3	25	183	188	Acetone	R141b	Cyclopentane

4. Results and Discussion

4.1   Case study based on PCM melting temperatures

The initial analysis involves a single stage compression in the HTHP and a simple ORC cycle, with no regeneration or recuperation. In Case 3, the effect of including two stages of compression in the HTHP was analyzed. This helps reducing the discharge temperature, however, the increase in the complexity of the system does not compensate the efficiency enhancements.
Apart from this, very similar trends were obtained for the three melting temperatures, so only Case 2 ($T_{melt} = 149°C$) is discussed in the following sections.

4.1.1. General cycle analysis

For the T-s analysis of the system, T_{source} was set to 70 °C. For this case, the melting temperature (149 °C) is near to the critical temperature of both R1233zd(E) and HFO1336mzz(Z). In **¡Error! No se encuentra el origen de la referencia.**, it is important to notice the difference in the slope of the saturated vapor line and the effect of the evaporation temperature. Since the dry fluid, HFO1336mzz(Z), has a positive slope of the saturation curve, a high degree of superheating is needed in order to prevent wet compression in the charging cycle, hereby leading to a lower evaporation temperature. This will significantly reduce the COP_{HTHP}. Moreover, for the expansion case it is clear that the degree of desuperheating in the ORC's condenser is very high. On the other hand, acetone's discharge temperature (after compression) is higher than in the other fluids Since the compression efficiency is assumed to be the same for all fluids, the negative slope of the vapor saturation curve causes a high discharge temperature, which may affect to the properties of the lubrication oil, damaging the compressor. R1233zd(E) is considered as an isentropic fluid but, since the slope of the saturated vapor line is slightly positive, a small amount of superheat at the outlet of HTHP's evaporator is needed in order to prevent the wet compression.
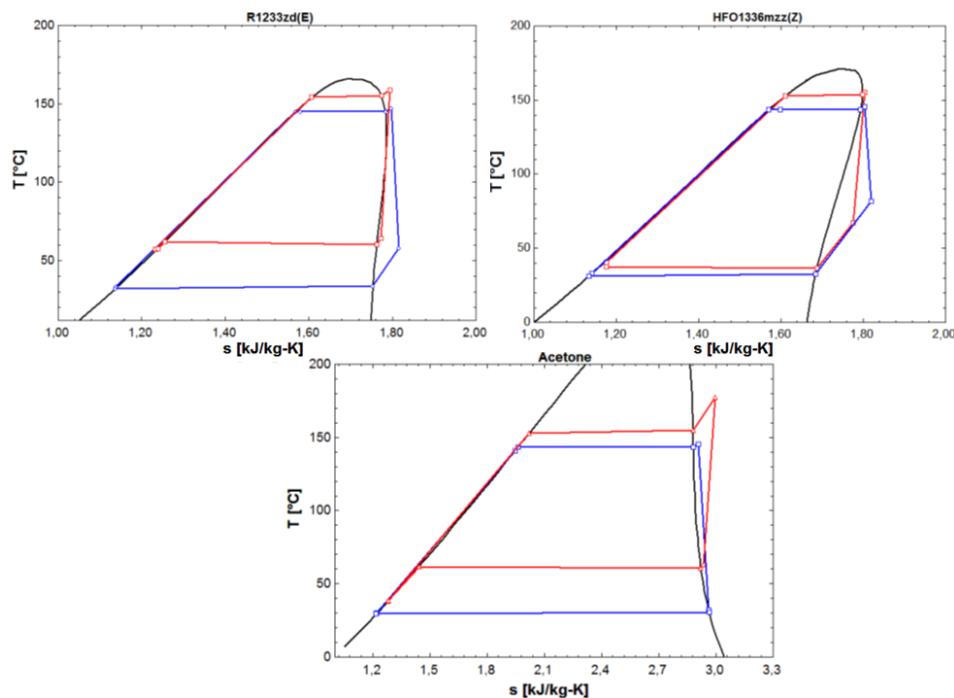

Figure 4. Representation of charging (red) and discharging (blue) cycles on T-s diagram for the working fluids selected for Case 2

4.1.2. Overall system performance

Figure 5 shows the roundtrip efficiency as a function of the source temperature (T_{source}). The general trend when the source temperature increases is an exponential increase of the roundtrip efficiency. However, for high source temperatures, the roundtrip efficiency is lower for all fluids. HFO1336mmz(Z) has a lower performance than the other fluids in the whole temperature range; this is due to the fact that dry fluids require high degrees of superheating. The roundtrip efficiencies of R1233zd(E) and Acetone are similar.

When comparing the three cases, the results show that, for high values of T_{source}, the roundtrip efficiency decreases when increasing $T_{melt.}$. For example, when $T_{source} = 100$ °C, R1233zd(E) has a roundtrip efficiency which is 11% lower in comparison to Case 1.
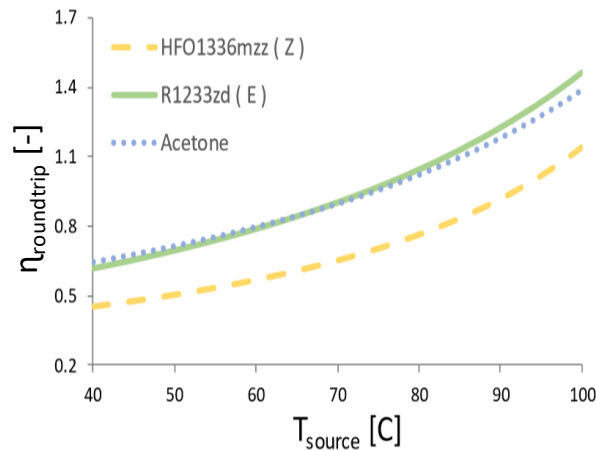
7

Figure 5. Roundtrip efficiency vs source temperature for CHEST system for Case 2

4.1.3. Heat pump cycle performance

Figure 6 shows the COP_{HTHP} as a function of the source temperature for Case 2. In accordance with the Carnot efficiency, the COP_{HTHP} is higher when the temperature lift is smaller. R1233zd(E) has the highest COP_{HTHP} and hence performs best out of the fluids, it reaches a COP_{HTHP} of 9.3 when $T_{source}=100$ °C. Since it is an isentropic fluid, the compressor work is the smallest compared to other two fluids.

In relation with Cases 1 and 3, as T_{melt} increases, the COP_{HTHP} decreases due to the increase of condensation temperature. For instance, for a $T_{source} = 100$ °C and the refrigerant R1233zd(E), COP_{HTHP} in Case 2 decreases by a 22% compared to Case 1.
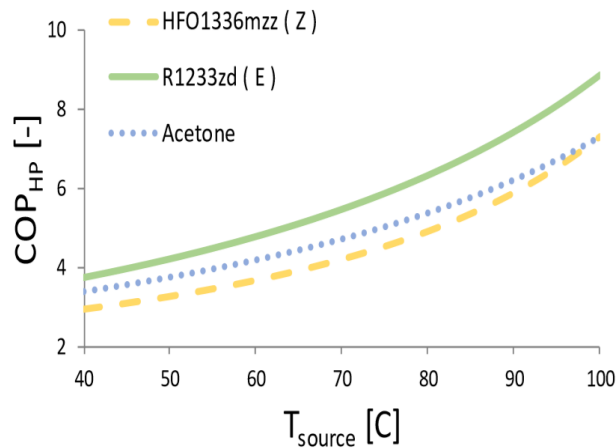

Figure 6. COP_{HTHP} vs T_{source} for Case 2

Figure 7 shows the VHC_{HTHP} as a function of the T_{source}. R1233zd(E) has the highest values of VHC_{HTHP} compared with others. Within the range of T_{source} studied, the average values of VHC_{HTHP} for R1233zd(E), Acetone, and HFO1336mzz(Z) are 4725, 1964, and 1476 kJ/m^3, respectively.
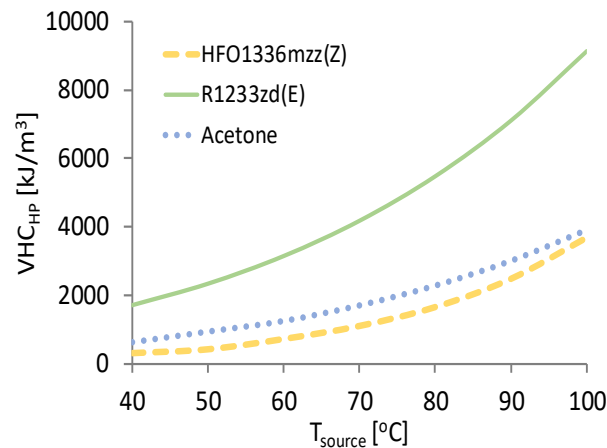
Figure 7. VHC$_{HTHP}$ vs T$_{source}$ for Case 2

4.1.4. Organic Rankine cycle performance

The η$_{thermal,ORC}$ and the VER$_{ORC}$ of the ORC can be seen in Figure 8 for each refrigerant was calculated at a constant T$_{source}$=70 °C. For given fixed melting and sink temperatures, both parameters remain constant when increasing the source temperature. HFO1336mzz(Z) has a low thermal efficiency in the ORC cycle. This is because, for a dry fluid, there is a high degree of superheat at the outlet of the expander. Acetone has the best thermal efficiency of the working fluids (≈19%) which is about 3% higher than for HFO1336mzz(Z).

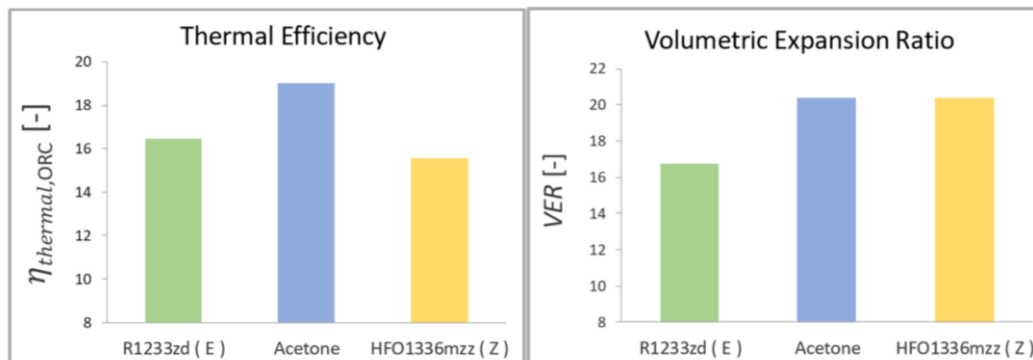Figure 8. Thermal efficiency and volumetric expansion ratio for the ORC for Case 2 at T$_{source}$=70 °C

As expected for an ORC cycle, the thermal efficiency is higher when T$_{melt}$ of the PCM is higher, as the discharging cycle reaches higher efficiencies with a larger temperature difference between the melting temperature and the sink temperature. The VER$_{ORC}$ is also larger at high values of T$_{melt}$. This is because the specific volume at the inlet of the expander is lower at high temperatures. For example, comparing Cases 1 and 2 for the isentropic refrigerant R1233zd(E) when T$_{source}$=100 °C, there is an increase of 8% in the η$_{thermal,ORC}$ and of 49% in the VER$_{ORC}$.

4.2 Effect of regeneration and recuperation on the ORC performance

This section shows the results of the roundtrip efficiency when recuperation and regeneration are included in the ORC. To see how the recuperation and vapor bleed affect the results, Case 2 with refrigerant R1233zd(E) was chosen and the source temperature was set to 70 °C. The main reasons for selecting R1233zd(E) are the reasonable roundtrip efficiency and low discharge temperature, compared with other fluids as seen in the previous section. Moreover, it has a low global warming potential (GWP) and is non-toxic. Therefore, it is most likely to be used in a real system.

4.2.1 ORC with regeneration

In this section, regeneration (vapor bleeding) in the ORC is activated while recuperation is kept deactivated. The thermal efficiencies and the temperature difference in the SHS are evaluated as a function of the regeneration pressure ratio or bleeding pressure (Eq. (*5*)). Figure 9 shows the effect of regeneration on the system performance.

$$P_{bleed}= r_P \times (P_6 - P_9) + P_9 \tag{5}$$

P_6 and P_9 (kPa) are the evaporation and condensation pressures of the ORC. The regeneration pressure ratio r_P (-) ranges from 0 to 1. This equation makes P_{bleed} (kPa) vary between the condensation pressure (when $r_P= 0$) and the evaporation pressure (when $r_P= 1$).
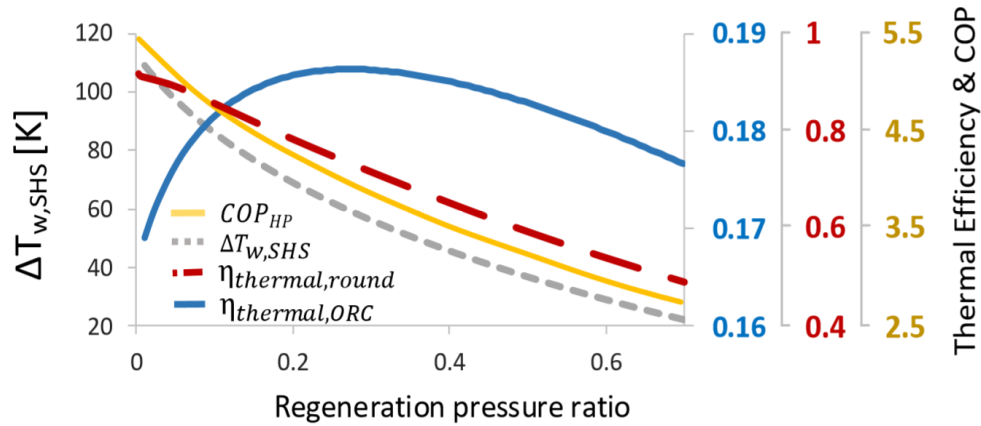

Figure 9. Effect of the regeneration process on the CHEST system performance

When the bleeding pressure is very close to the condensation pressure (i.e pressure ratio ≈ 0), the roundtrip efficiency is the same as in the simple ORC case. When the pressure ratio increases, the preheating of the working fluid increases, leading to an increase in the inlet temperature to the SHS on the ORC-side. The water temperature difference between the inlet and outlet of the SHS ($\Delta T_{w,SHS}$) decreases in order to prevent a violation of the second law of thermodynamics. Figure 9 also shows that the thermal efficiency of the ORC has a maximum value when the pressure ratio is equal to 0.25. This is because on the one side, the loss of mass flow in the expander reduces the work output in the expander and thereby the thermal efficiency. One the other side, it has to be weighted with the increase in the preheating, which has a favorable effect on the thermal efficiency. The COP$_{HTHP}$ reduced because regeneration in the ORC side implies lower subcooling, which means a lower stored heat and, subsequently, a lower COP$_{HTHP}$. Since the compression work from the heat pump is constant, the roundtrip efficiency is reduced because the work output from the expansion is reduced. The work output is reduced due to the loss in the mass flow rate of the second stage expansion.

4.2.2 ORC with recuperation

In this section, the recuperation process in the ORC is activated, while the regeneration is deactivated. Figure 10 the effect of the recuperation process on the $\eta_{roundtrip}$, $\eta_{thermal,ORC}$, COP$_{HTHP}$, and $\Delta T_{w,SHS}$. As the recuperator effectiveness increases, the outlet temperature of the recuperator increases, which also means that the refrigerant temperature at the inlet of the SHS will increase. Therefore, the $\Delta T_{w,SHS}$ should be decreased in order prevent a violation of the second law of thermodynamics. The $\eta_{thermal,ORC}$ increases when adding a recuperator, due to the additional heat recovery. However, Figure 10 also shows that the COP$_{HTHP}$ decreases when increasing the effectiveness of the recuperator. The explanation for this is that the subcooling in the heat pump cycle decreases when more heat is recovered in the ORC. The total roundtrip efficiency remains

constant no matter the recuperator effectiveness because the efficiency gain in the ORC is reduced by the efficiency loss in the HTHP.
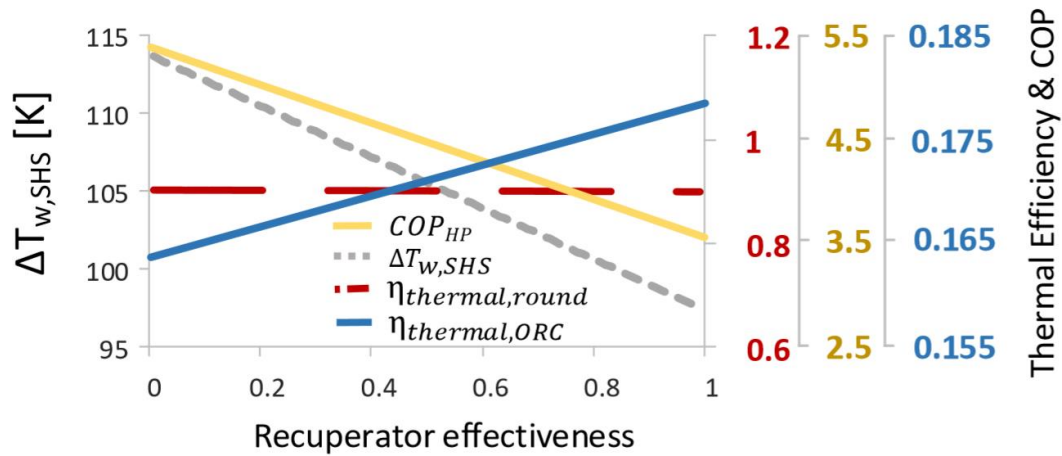

Figure 10. Impact of recuperation process on the CHEST system performance

5. Conclusions and Future Work

This work has focused on building a thermodynamic model of a heat energy storage system and optimizing it by comparing different working fluids and system layouts. Although the work is in an early phase, some remarks can already be drawn regarding the general system configuration and the potential working fluids.

As a general conclusion, the results of the three cases studied indicate that isentropic fluids are preferable for the CHEST system. Dry fluids require high superheat in the HTHP's evaporator to prevent wet compression, which subsequently reduces the roundtrip efficiency; wet fluids result in high discharge temperatures, which can affect the performance of lubrication oil and damage the compressor. Using isentropic fluids (R1233zd(E) in Cases 1 and 2, and R141b in Case 3), a 100% roundtrip efficiency can be reached at source temperatures of 74, 80 and 100 ºC for Cases 1, 2 and 3, respectively. This indicates that the CHEST system could be a competitive and therefore promising thermal energy storage alternative. Also, isentropic fluids have high VHC_{HTHP} and low VER_{ORC} values, which, respectively, are indicators of small compressor and expander sizes.

The effect of recuperation and regeneration in the cycle has also been analyzed. The most important conclusion is that it is not beneficial for the roundtrip efficiency to include regeneration or recuperation processes in the CHEST system. This conclusion is valid as long as most of the subcooled liquid in the HTHP is used for the SHS and later, to preheat the ORC.

As future work, the dynamics of the CHEST system will be analyzed by developing a transient model, which enables the system to charge and discharge at different times and working conditions, as well as taking into account the heat losses in the thermal storage.

Acknowledgements

REFERENCES

[1]   ANEKE, M; WANG, M. *Energy storage technologies and real life applications – A state of the art review*. *Applied Energy*. 2016, **179**, 350–377.

[2]   DINKER, A; AGARWAL, M; AGARWAL, G D. *Heat storage materials, geometry and applications: A review*. *Journal of the Energy Institute*. 2017, **90**(1), 1–11.

[3]   GUO, J; CAI, L; CHEN, J; ZHOU, Y. *Performance optimization and comparison of pumped thermal and pumped cryogenic electricity storage systems*. *Energy*. 2016, **106**, 260–269.

[4]   JOCKENHÖFER, H; STEINMANN, W D; BAUER, D. *Detailed numerical investigation of a pumped thermal energy storage with low temperature heat integration*. *Energy*. 2018, **145**, 665–676.

[5]   KLEIN, S . *Engineering Equation Solver; (Version V10.451), F-Chart Software*. 2018.

[6]   PEREIRA DA CUNHA, J; EAMES, P. *Thermal energy storage for low and medium temperature applications using phase change materials - A review*. *Applied Energy*. 2016, **177**, 227–238.

[7]   VANKEIRSBILCK, I; VANSLAMBROUCK, B; GUSEV, S. *Energetical , Technical and Economical considerations by choosing between a Steam and an Organic Rankine Cycle for Small Scale Power Generation 2 . The Steam Cycle 3 . The Organic Rankine Cycle 4 . Benchmark ORC vs Steam*. *Prezentacja*. 2011.

[8]   WANG, D; LING, X; PENG, H; LIU, L; TAO, L L. *Efficiency and optimal performance evaluation of organic Rankine cycle for low grade waste heat power generation*. *Energy*. 2013, **50**(1), 343–352.

[9]   WELZL, M; HEBERLE, F; BRÜGGEMANN, D. *Simultaneous experimental investigation of nucleate boiling heat transfer and power output in ORC using R245fa and R1233zd(E)*. *Energy Procedia*. 2017, **129**, 435–442.

[10]   WOODLAND, B J; KRISHNA, A; GROLL, E A; BRAUN, J E; HORTON, W T; GARIMELLA, S V. *Thermodynamic comparison of organic Rankine cycles employing liquid-flooded expansion or a solution circuit*. *Applied Thermal Engineering*. 2013, **61**(2), 859–865.

[11]   *Statistical Review of World Energy | Home | BP*. [accessed. 2019-01-24]. Available at: https://www.bp.com/en/global/corporate/energy-economics/statistical-review-of-world-energy.html

[12]   *Compressed Heat Energy Storage for Energy from Renewable sources | Projects | H2020 | CORDIS | European Commission*. [accessed. 2018-07-05]. Available at: https://cordis.europa.eu/project/rcn/214061/factsheet/en

[13]   *Consortium » CHESTER Project*. [accessed. 2019-01-24]. Available at: https://www.chester-project.eu/consortium/

[14]   *R1336mzz-Z - new generation nonflammable low GWP refrigerant | KTH*. [accessed. 2019-01-24]. Available at: https://www.kth.se/en/itm/inst/energiteknik/forskning/ett/projekt/koldmedier-med-lag-gwp/low-gwp-news/r1336mzz-z-ett-nytt-hogtemperaturkoldmedium-med-bra-egenskaper-1.501202